Journal of Alloys and Compounds 506 (2010) 323–326

Contents lists available at ScienceDirect

Journal of Alloys and Compounds

journal homepage: www.elsevier.com/locate/jallcom

Effects of MnO doping on properties of $0.97K_{0.5}Na_{0.5}NbO_3$–$0.03(Bi_{0.5}K_{0.5})TiO_3$ piezoelectric ceramics

X.P. Jiang[a], Y. Chen[a,b,*], K.H. Lam[b], S.H. Choy[b], J. Wang[b]

[a] Department of Materials Science and Engineering, Jingdezhen Ceramic Institute, Jingdezhen 333001, China
[b] Department of Applied Physics and Materials Research Center, The Hong Kong Polytechnic University, Hong Kong, China

ARTICLE INFO

Article history:
Received 28 January 2010
Received in revised form 24 June 2010
Accepted 30 June 2010
Available online 13 July 2010

Keywords:
Lead-free piezoelectric ceramics
MnO doping
Electric properties

ABSTRACT

MnO-doped $0.97K_{0.5}Na_{0.5}NbO_3$–$0.03(Bi_{0.5}K_{0.5})TiO_3$ lead-free piezoelectric ceramics have been fabricated by solid state reaction. The MnO-doped KNN-BKT samples show tetragonal perovskite structure and the grain size increases obviously. With an addition of the optimal doping of MnO, all the electrical properties of the samples, especially the piezoelectric and pyroelectric performance, have been enhanced significantly. The KNN-BKT ceramics, with 0.8 wt% MnO doping, exhibits optimal electrical properties: d_{33} = 221 pC/N, k_p = 44.7%, $tg\delta$ = 1.4%, ε_r = 1229, Q_m = 143, ρ = 4.464 g/cm^3 and p = 221 μC/m^2 K.

1. Introduction

In recent years, the most widely used piezoelectric materials are lead-based PZT ceramics due to their excellent electric properties. However, the application of the lead-based ceramics would cause serious environment problems, for example, the wasting products containing Pb in the earth lead to contaminate the ground water by acid rain. Therefore, the investigation of the lead-free piezoelectric ceramics has been attracted much attention, especially for the perovskite structure $(K_{0.5}Na_{0.5})NbO_3$ (KNN)-based piezoelectric ceramics due to their excellent piezoelectric properties and high Curie temperature [1]. Nevertheless, it is extremely difficult for pure KNN to achieve high density by using an ordinary sintering method [2,3]. Thus, extensive studies have been carried out to improve the sintering performance and properties of KNN ceramics. Oxide dopants, such as ZnO [4], CuO [4,5], MnO_2 [4–7], MnO [8], were used to improve the properties of KNN. Besides, $Li_{0.5}Bi_{0.5}TiO_3$ [9] $BiScO_3$ [10], $Ba(Zr_{0.05}Ti_{0.95})O_3$ [11], $CaTiO_3$ [12], $LiNbO_3$ [13], $Bi(Zn_{0.5}Ti_{0.5})O_3$ [14], $BiAlO_3$ [15], and $(Bi_{0.5}K_{0.5})TiO_3$ [16] have been studied to add into the KNN to form new solid solutions. Among these, $(Bi_{0.5}K_{0.5})TiO_3$ (BKT) is a well known tetragonal ferroelectric material with high Curie temperature (T_c = 380 °C), which has been widely used in ceramic technology [17,18]. By hot pressing sintering method, the coercive field E_c and remnant polarization P_r of the BKT were reported to be 20.7 kV/cm and 5.4 μC/cm^2, respectively. The electromechanical planar coupling coefficient k_p was 15.2, and the piezoelectric constant d_{33} was 69.8 pC/N [19]. With the addition of BKT, KNN-$(Bi_{0.5}K_{0.5})TiO_3$ [16] (KNN-BKT) ceramics possess a high piezoelectric d_{33} constant of 192 pC/N which was obtained by high-energy attrition milling. In order to further improve the properties of KNN-BKT ceramics, Mn was doped by solid state reactions. The microstructural and electrical properties of the Mn-doped ceramics are investigated in this paper.

2. Experimental

The samples were prepared according to the formula: $0.97K_{0.5}Na_{0.5}NbO_3$–$0.03(Bi_{0.5}K_{0.5})TiO_3$ + x wt% MnO ($0 \le x \le 2$) (abbreviated as KNN-BKT + xMnO), where x = 0, 0.4, 0.8, 1, 1.5, and 2, respectively. Reagent-grade oxide and carbonate powders of K_2CO_3, Na_2CO_3, Nb_2O_5, Bi_2O_3, TiO_2 and $MnCO_3$ were used as starting materials. The powders were weighed and mixed by ball-milling in alcohol for 6–8 h. After drying, the powders were calcined at 850 °C for 2 h. The calcined powders were mixed again and pressed into discs. The disc samples were then sintered in air in the temperature range of 1050–1100 °C for 2 h, depending on x. Both surfaces of the sample were coated with silver paste as electrodes and polarized under a DC field of 4 kV/mm at 80 °C in silicone oil for 15–20 min. The crystalline structure of sintered samples was identified by an X-ray diffractometer (D8 Advanced, Bruker). The scan step is 0.02° and the time interval is 1 s. The lattice parameters were calculated according to the Bragg diffraction [20]. The microstructure was observed using a scanning electron microscopy (SEM) (JSM-6700F, JEOL). The bulk density ρ was measured by the Archimedes method. The piezoelectric constant d_{33} was measured using a piezo-d_{33} meter (ZJ-3A, Institute of Acoustics, Chinese Academy of Sciences, Beijing). The mechanical quality factor and the electromechanical coupling factor of the samples were determined following the IEEE standard on piezoelectricity [21] by measuring the resonant and anti-resonant frequencies using an impedance analyzer (Agilent 4294A, Agilent Technology Inc.). Dielectric properties as a function of temperature were also measured by an impedance analyzer (Agilent 4294A). The room temperature polarization–electric field (P–E) hysteresis loops were measured using a modified

* Corresponding author.
E-mail address: yanchen83@hotmail.com (Y. Chen).

0925-8388/$ – see front matter © 2010 Elsevier B.V. All rights reserved.
doi:10.1016/j.jallcom.2010.06.200

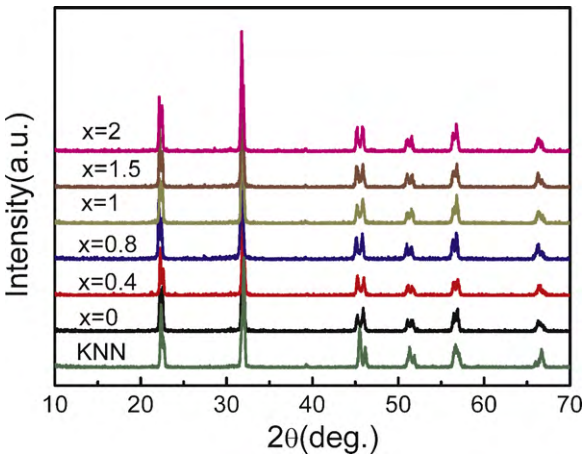

Fig. 1. XRD patterns of KNN ceramics and KNN-BKT + *x*MnO ceramics.

Sawyer Tower circuit at 10 Hz. The pyroelectric coefficient *p* was measured by the dynamic method [22].

3. Results and discussion

The XRD patterns of all the KNN-BKT + *x*MnO samples with different *x* are shown in Fig. 1. Compared with the orthorhombic perovskite structure of the pure KNN ceramic [11], the KNN-BKT + *x*MnO samples possess a pure tetragonal perovskite structure without showing any other secondary phase. This indicates that MnO has diffused into the KNN-BKT lattices and the crystal structure of the KNN-BKT + *x*MnO samples would not change obviously by doping a small amount of MnO [23]. Since the ionic radius of Mn^{2+} (0.83 Å) and Mn^{3+} (0.645 Å) is much smaller than that of A-site ions (K^+: 1.38 Å, Na^+: 1.02 Å, Bi^{3+}: 1.03 Å), Mn ions are more likely to substitute into B-site ions (Ti^{4+}: 0.605 Å, Nb^{5+}: 0.64 Å, CN = 6) [24]. Mn^{2+} or Mn^{3+} ions substituting for B-site Ti^{4+} or Nb^{5+} causes the formation of oxygen vacancies so that the lattice may have a small shrinkage. Nevertheless, the lattice still grows because of different ionic sizes which can compensate the shrinkage of the lattice. Therefore, there is no obvious change on the XRD patterns of the samples with different *x* (Fig. 1) [23]. The lattice parameters of the KNN-KBT ceramics are given in Table 1 to show the asymmetric characteristics of the unit cell. It is shown that the unit cell increases with Mn doping, while $x \geq 1.5$, the lattice parameters remain unchanged which indicates that the solubilization limit has already reached.

Fig. 2 shows the relative density of the sintered KNN-BKT + *x*MnO ceramics as a function of *x*. High relative density (>97%) of the ceramics was obtained. After MnO doping, the density increases slightly. Fig. 3 shows SEM micrographs of the

Table 1
Lattice parameters of KNN-KBT + *x*MnO ceramics.

x (wt%)	*a* = *b* (Å)	*c* (Å)
0	4.002	3.948
0.4	4.002	3.941
0.8	4.012	3.956
1	4.009	3.951
1.5	4.004	3.951
2	4.004	3.951

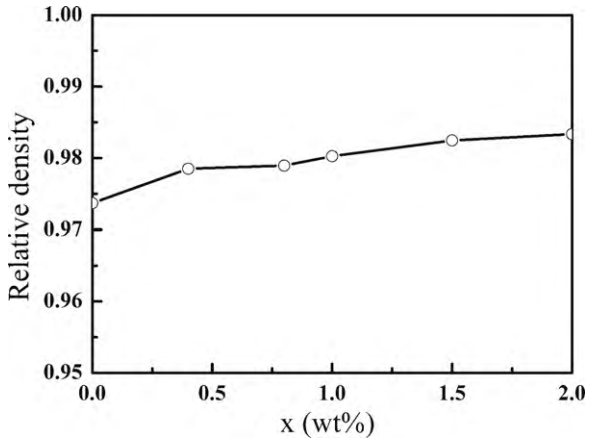

Fig. 2. Relative density of KNN-BKT + *x*MnO ceramics.

KNN-BKT + *x*MnO samples. For the pure KNN-BKT ceramic ($x = 0$), the grain size is in the range of 0.3–1 μm. With increasing *x*, the grain size is about 2 μm in average. It can be seen that the grain growth becomes inhomogeneous when the amount of *x* exceeds 0.8. Similar phenomenon was observed in MnO doped $0.95Na_{0.5}K_{0.5}NbO_3$–$0.05LiTaO_3$ ceramics [8].

Besides the microstructure, MnO doping also affects the piezoelectric properties of KNN-BKT + *x*MnO ceramics significantly. It was reported that after MnO doping, the enhancement of density and grain size can improve the piezoelectric performance [25]. Fig. 4 shows the MnO dependence on the piezoelectric and dielectric properties of the KNN-BKT + *x*MnO ceramics. Piezoelectric constant (d_{33}), electromechanical planar coupling coefficient (k_p) and the relative permittivity (ε_r) (1 kHz) increase firstly for *x* up to 0.8 and then decrease with further increasing MnO amount. It may be due to the inhomogeneous grain growth when the doping amount exceeds 0.8 wt%. The results show that the performance of the ceramics is sensitive to the doping amount. The properties degrade when the doping amount of MnO exceeds 0.8 wt%.

Due to the B-site substitution of Mn ions, oxygen vacancies exist to enhance the mechanical quality factor (Q_m) and decrease the loss tangent ($tg\delta$), which indicates that the doping of MnO causes "hard

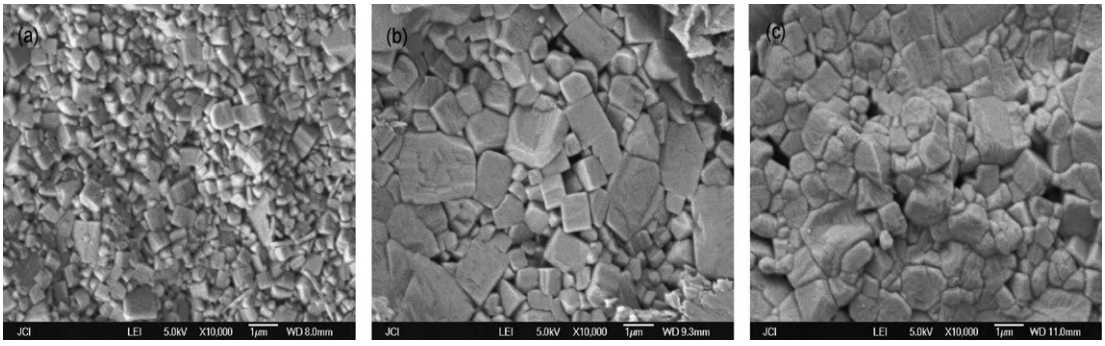

Fig. 3. SEM micrographs of KNN-BKT + *x*MnO ceramics with (a) $x = 0$, (b) $x = 0.8$ and (c) $x = 2$.

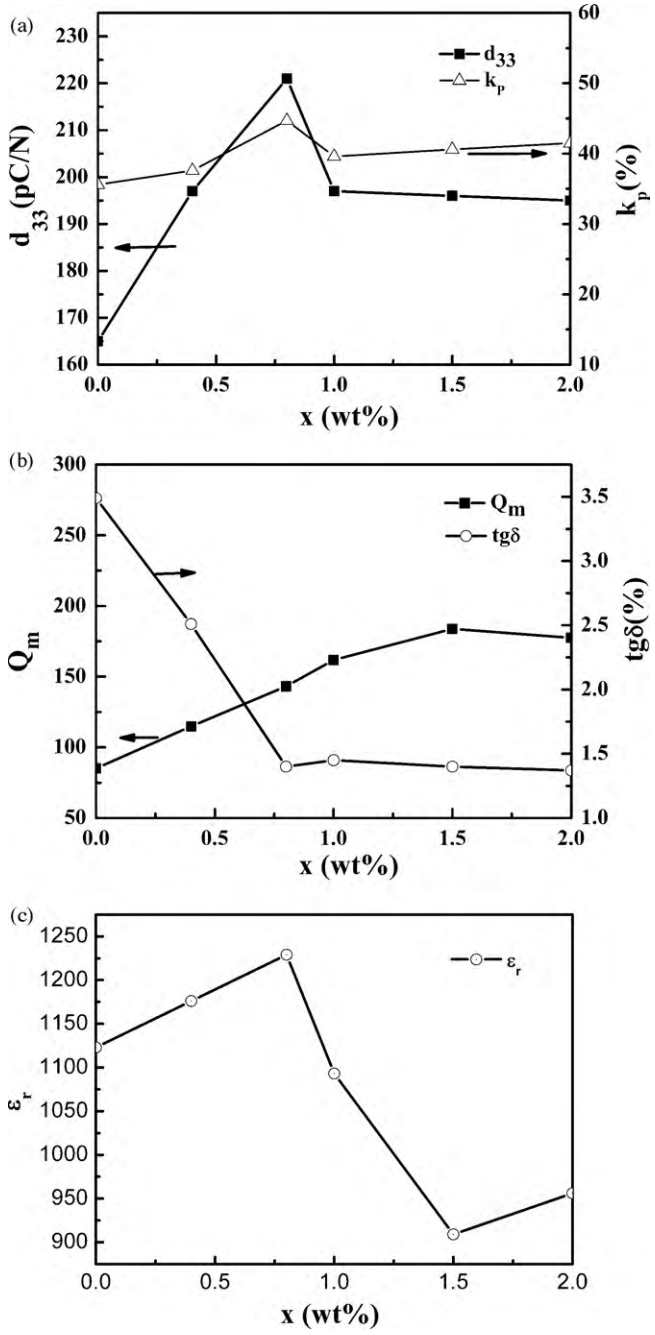

Fig. 4. Electrical properties of KNN-BKT + *x*MnO ceramics.

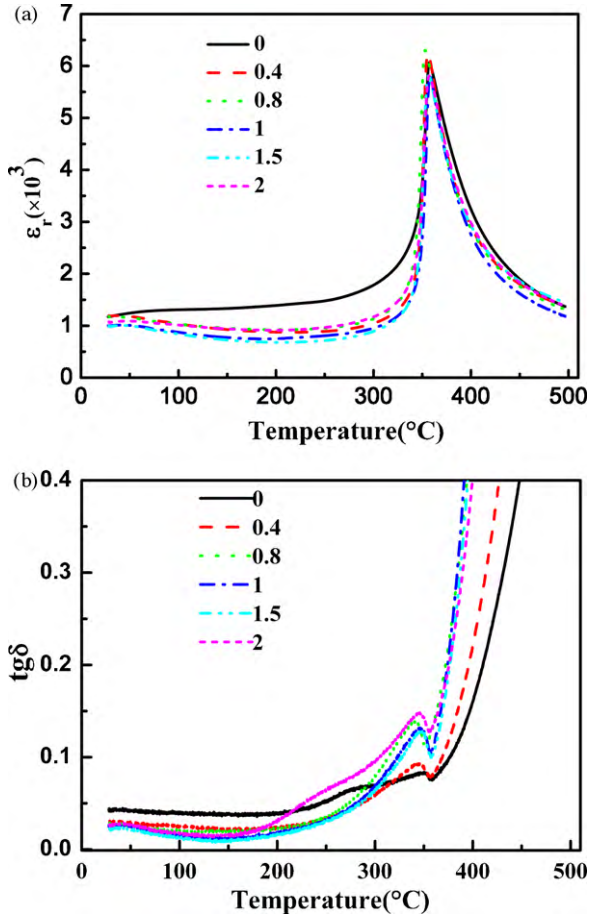

Fig. 5. Temperature dependence of the relative permittivity and loss tangent for the unpoled KNN-BKT + *x*MnO ceramics at 10 kHz.

doping" effect in the KNN-BKT + *x*MnO ceramics. As shown in the SEM micrographs, the grain size of the ceramics increases after MnO doping so that the relative permittivity (ε_r) would also increase as well [25].

The temperature dependence of relative permittivity and loss tangent at 10 kHz for KNN-BKT + *x*MnO is shown in Fig. 5. All samples show only one dielectric peak at about 350 °C, which corresponds to the Curie temperature (T_C). The loss tangent of all samples is smaller than 5% from room temperature to 200 °C and with a peak at the Curie temperature. The further rapid increase of the loss beyond the Curie temperature is due to the conductive losses [13].

In order to study the effect of MnO content on the ferroelectric properties, the room temperature *P*–*E* hysteresis loops of the KNN-BKT + *x*MnO ceramics as a function of *x* were measured at 10 Hz as shown in Fig. 6. When $x = 0.8$, there is no obvious effect on E_c and P_r when comparing with the ceramics of $x = 0$. For further increasing *x*, poor ferroelectric performance is observed as P_r decreases and E_c increases.

Table 2 compares the pyroelectric coefficient, dielectric properties and the figures of merit of KNN-BKT + *x*MnO ceramics. Three major figures of merit (FOMs) are listed in the table: current responsivity $F_i = p/C_v$, voltage responsivity $F_v = p/(C_v\varepsilon_0\varepsilon_r)$, and detectivity $F_d = p/[C_v(\varepsilon_0\varepsilon_r tg\delta)^{1/2}]$, where p, $C_v = \rho C_p$, C_p, ε_0, ε_r, and $tg\delta$ are the pyroelectric coefficient, volume specific heat, mass specific heat,

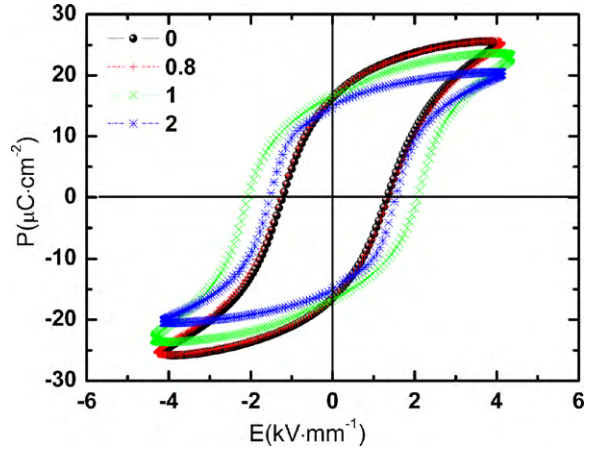

Fig. 6. *P*–*E* hysteresis loops of KNN-BKT + *x*MnO ceramics.

Table 2
List of pyroelectric coefficient, dielectric properties, and figures of merits for KNN-BKT + xMnO ceramics.

x (wt%)	ε_r (at 100 Hz)	$tg\delta$ (at 100 Hz)	ρ (kg/m^3)	C_p (J/kg K)	p (μC/m^2 K)	F_i (pm/V)	F_v (m^2/C)	F_D (μPa$^{1/2}$)
0	1159	0.033	4440	545.69	101	41.6	0.0041	2.26
0.4	1176	0.037	4462	545.33	179	73.6	0.0071	3.75
0.8	1277	0.031	4464	549.65	221	90.07	0.008	4.81
1	1144	0.034	4470	522	197	84.42	0.008	4.55
2	980	0.035	4484	488.95	218	99.4	0.0114	5.71

the permittivity of free space (=8.85 × 10^{-12} F/m), relative permittivity, loss tangent, respectively [21]. As shown in the table, the p coefficient and the FOMs of KNN-BKT ceramics have been improved after MnO doping. Similar to the piezoelectric properties, the sample with x = 0.8 has the best pyroelectric performance among the doped samples, which doubles the p coefficient compared to pure KNN-BKT ceramics. Hence, Mn doping is suggested as an effective way to enhance both the pyroelectric and piezoelectric properties of KNN-BKT ceramics.

4. Conclusions

Lead-free piezoelectric KNN-BKT + xMnO ceramics have been synthesized by solid state reaction. The effect of MnO content on the piezoelectric, dielectric, ferroelectric and pyroelectric properties of the KNN-BKT ceramics has been studied. With the addition of MnO, no significant improvement on ferroelectric performance is observed. Nevertheless, the piezoelectric, dielectric and pyroelectric properties have been enhanced greatly with MnO doping. It was also found that the performance of the ceramics is sensitive to the MnOdoping amount. The KNN-BKT + xMnO ceramic with x = 0.8 exhibits the optimal properties: d_{33} = 221 pC/N, k_p = 44.7%, $tg\delta$ = 1.4%, ε_r = 1229, Q_M = 143, ρ = 4.464 g/cm^3 and p = 221 μC/m^2 K.

Acknowledgements

This work was supported by National Natural Science Foundation of China (Grant No: 50862005, 50562002), the New Century Excellent Talents in University (Grant No: NCET-06-0576), the Jiangxi Natural Science Foundation and Cooperative Project (Grant No: 2007GZC1258, 2007GZC1258, 2008-212), the Jiangxi Colleges and Universities “advanced ceramics” scientific and technological innovation team. Thanks are also to the Centre for Smart Materials of The Hong Kong Polytechnic University.

References

[1] Y. Saito, H. Takao, T. Tani, T. Nonoyama, K. Takatori, T. Homma, T. Nagaya, M. Nakamura, Nature 432 (2004) 84.
[2] M.D. Maeder, D. Damjanovic, N. Setter, J. Electroceram. 13 (2004) 385.
[3] W.W. Wolny, Ceram. Int. 30 (2004) 1079.
[4] W. Yang, D. Jin, T. Wang, J. Cheng, Physica B 405 (2010) 1918.
[5] D. Lin, K.W. Kwok, H.L.W. Chan, J. Alloy Compd. 461 (2008) 273.
[6] D. Lin, Q. Zheng, K.W. Kwok, C. Xu, C. Yang, J. Mater. Sci: Mater. Electron. 21 (2010) 649.
[7] D. Lin, K.W. Kwok, H. Tian, H.L.W. Chan, J. Am. Ceram. Soc. 90 (5) (2007) 1458.
[8] P. Bomlai, P. Sinsap, S. Muensit, S. Milne, J. Am. Ceram. Soc. 91 (2) (2008) 624.
[9] X. Jiang, Q. Yang, Z. Yu, F. Hu, C. Chen, N. Tu, Y. Li, J. Alloy Compd. 493 (2010) 276.
[10] X. Li, J. Zhu, M. Wang, Y. Luo, W. Shi, L. Li, J. Zhu, D. Xiao, J. Alloy Compd. 499 (2010) L1–L4.
[11] D. Lin, K.W. Kwok, H.L.W. Chan, Appl. Phys. Lett. 91 (2007) 143513.
[12] J. Wu, D. Xiao, Y. Wang, J. Zhu, W. Shi, W. Wu, B. Zhang, J. Li, J. Alloy Compd. 476 (2009) 782.
[13] Y. Guo, K. Kakimoto, H. Ohsato, Appl. Phys. Lett. 85 (2004) 4121.
[14] M. Sutapuna, C. Huang, D.P. Cann, N. Vittayakorna, J. Alloy Compd. 479 (2009) 462.
[15] R. Zuo, D. Lv, J. Fu, Y. Liu, L. Li, J. Alloy Compd. 476 (2009) 836.
[16] R. Zuo, X. Fang, C. Ye, L. Li, J. Am. Ceram. Soc. 90 (8) (2007) 2424.
[17] C.F. Buhrer, J. Chem. Phys. 36 (1962) 798.
[18] T. Wada, A. Fukui, Y. Matsuo, Jpn. J. Appl. Phys. 41 (2002) 7025.
[19] Y. Hiruma, R. Aoyagi, H. Nagata, T. Takenaka, Jpn. J. Appl. Phys. 44 (7A) (2005) 5040.
[20] C. Hammond, The Basics of Crystallography and Diffraction, Oxford University Press, Now York, 2001.
[21] IEEE Standard on Piezoelectricity, ANSI/IEEE Std. 176 (1987).
[22] S.T. Lau, C.H. Cheng, S.H. Choy, D.M. Lin, K.W. Kwok, H.L.W. Chan, J. Appl. Phys. 103 (2008) 104105.
[23] R.Z. Zuo, Z.K. Xu, L.T. Li, J. Phys. Chem. Solids 69 (2008) 1728.
[24] R.D. Shannon, Acta Cryst. A 32 (1976) 751.
[25] M. Zhu, L. Liu, Y. Hou, H. Wang, H. Yan, J. Am. Ceram. Soc. 90 (1) (2007) 120.